MATHEMATICAL MODEL AND EXPERIMENTAL STUDY OF AIRFLOW IN SOLAR CHIMNEYS

Zoltan Adam, Toshio Yamanaka and Hisashi Kotani

Department of Architectural Engineering,
Graduate School of Engineering, Osaka University, Osaka, Japan, adamzoli@arch.eng.osaka-u.ac.jp

Summary
A detailed mathematical simulation and experimental investigation of airflow in solar chimneys is introduced in this paper. During the experiments the air speed in the chimney was found to be dependent on the distance from the heated plate, and if the glazing was installed far enough from the wall, the flow could not reach the glazing, decreasing the flow rate. This phenomenon was considered when the simulation model was set up. The results of the experiments and simulation are presented in series of graphs.

Introduction
The solar chimney discussed in this paper is a simple channel glazed on one side with a collector wall on the other. There are many models available to calculate the mass flow rate of such chimneys. Most of these models (Bansal et al. 1993, Sandberg et al. 1996, Alfonso et al. 2000) use average temperatures and heat transfer coefficients to calculate the temperature distribution inside the chimney. The calculation is based on the assumption that the dissipation of heat into the flowing fluid is uniform and there is no temperature distribution of the flowing air normal to the chimney wall.
In the recent study, series of experiments were conducted, and it was found that the air temperature distribution normal to the wall has a significant effect on the chimney's airflow rate. Also, different wall materials can influence the performance due to their radiation heat loss, so it was considered, too.

Numerical method
Dividing the chimney into a large number of blocks from the bottom to the top, a multi-zone model can be constructed. The model takes the buoyancy effect, friction losses, radiation, convective and conductive heat transfers into account. When radiation heat transfers arc calculated, the glazing is not divided into blocks, as the temperature of the glazing is almost uniform, and a great number of the resulting

equations would not be easy to solve. In order to simulate the flow pattern, the flowing fluid in the channel is divided into three separate layers (a, b and c) parallel to the wall.

Fluid temperature equations
If uniform dissipation of the convected heat is assumed, the following differential equation can be set up for the flowing fluid:

$$mc_p \frac{dT_f}{dx} \Delta x = h_f \left(T_w - T_f \right) w \Delta x \qquad (1)$$

where T_f, T_w, h_f is the fluid and wall temperature, and wall heat transfer coefficient. This equation can be modified to suit the block model. As the fluid in the channel is divided into layers, the number of layers that are involved in the heat transfer must be calculated. The boundary layer thickness is calculated the following way:
Equation for boundary layer thickness of a vertical plate turbulent flow (Katsuto 1964):

$$\delta_{t(x)} = \frac{0.58}{\mathrm{Pr}^{8/15}} \left(\frac{1 + 0.494\,\mathrm{Pr}^{2/3}}{Gr_{(x)}} \right)^{1/10} \qquad (2)$$

This equation must be altered to suit the real conditions: the variable channel thickness and inclination:

$$\delta_{t(x)} = \frac{s^A}{B sin^C \varphi} \frac{0.58}{\mathrm{Pr}^{8/15}} \left(\frac{1 + 0.494\,\mathrm{Pr}^{2/3}}{Gr_{(x)}} \right)^{1/10} \qquad (3)$$

The boundary layer was assumed to be the line where the fluid temperature reaches 1 K difference from the inlet temperature. In that case, suitable constants are:
    A=1/3, B=0.6, C=2.
Changing the differential equation to suit the block model, the following can be written:
When the thermal boundary does not reach a new layer, the following equation can be used to calculate the temperatures in layer (a) for a given block (i):

$$T_{fa(i)} = \frac{T_{fa(i-1)} m_a c_p + T_{w(i)} h_{(wf)(i)} \frac{wL}{n}}{m_a c_p + h_{(wf)(i)} \frac{wL}{n}} \qquad (4)$$

If there is a new layer (b) that is inside the thermal boundary of the flow, the following form should be used:

$$T_{fa(i)} = T_{fb(i)} = \frac{(m_a T_{fa(i-1)} + T_r m_b)c_p + \frac{wL}{n}h_{(wf)(i)}T_{w(i)}}{c_p(m_a + m_b) + h_{(wf)(i)}\frac{wL}{n}} \quad (5)$$

where $m_a; m_b$ is the mass flow inside the boundary in the previous block, and the mass flow of the layer that joins the heat transfer in the recent one. All the layers inside the boundary will have the same fluid temperature from that block on. See Figure 1 for details of the division and fluid temperature.
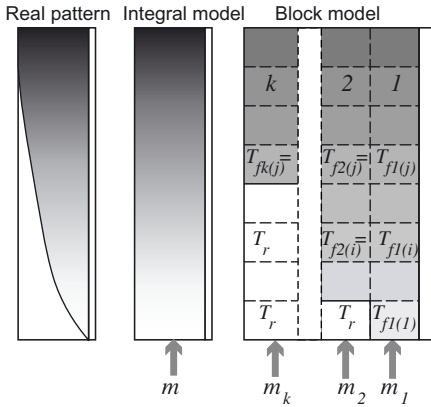

Figure 1. Simulation models

Local heat transfer coefficients
Local heat transfer coefficients at the wall can be calculated the following way (Holman 1997):

$$h_{(wf)(i)} = \frac{k}{L(i/n)}0.1\sqrt[3]{Gr\,\mathrm{Pr}} \quad (6)$$

where $Gr = \dfrac{(T_{w(i)} - T_r)(Li/n)^3 g\beta}{v^2}$, T_r is the room temperature.

Based on experimental observations, turbulent flow pattern was assumed at the wall.

Heat transfer equations
To calculate the variables in the fluid temperature equation, thermal balance equations for the wall and the glazing must be written up.
Heat balance for the glazing:

$$\sum_{i=1}^{n} q_{r(ge)(i)} + \sum_{i=1}^{n} q_{c(ge)(i)} = \sum_{i=1}^{n} q_{a(sg)(i)} + \sum_{i=1}^{n} q_{r(wg)(i)} \quad (7)$$

The parts of this equation can be written as:
Energy loss by radiation:

$$q_{r(ge)(i)} = \frac{\left(\overline{T_g}^4 - T_e^4\right)\sigma}{R_{(ge)}A_{g(i)}} \quad (8)$$

Where $R_{(ge)} = \dfrac{r_g}{\varepsilon_g A_{g(i)}} + \dfrac{1}{A_{g(i)}F_{(ge)}}$, $A_{g(i)} = wL/n$,

and $F_{(ge)} = 1$

Energy loss by convection to the environment:

$$q_{c(ge)(i)} = h_{(ge)}\left(\overline{T_g} - T_e\right) \quad (9)$$

Energy gain from the incident solar radiation:

$$q_{a(sg)(i)} = q_s \alpha_g \quad (10)$$

Energy gain from a block of wall by radiation:

$$q_{r(wg)(i)} = \frac{\left(T_{w(i)}^4 - \overline{T_g}\right)\sigma}{R_{(wg)}A_{g(i)}} \quad (11)$$

where $R_{(wg)}$ can be calculated as:

$$R_{(wg)} = \frac{1-\varepsilon_w}{\varepsilon_w A_{w(i)}} + \frac{1}{A_{w(i)}F_{(wg)}} + \frac{1-\varepsilon_g}{\varepsilon_g A_g}$$

$A_w = wL/n$, and it can be assumed that $F_{(wg)} \approx 1$, as the area of the glazing is huge compared to the area of a wall block.
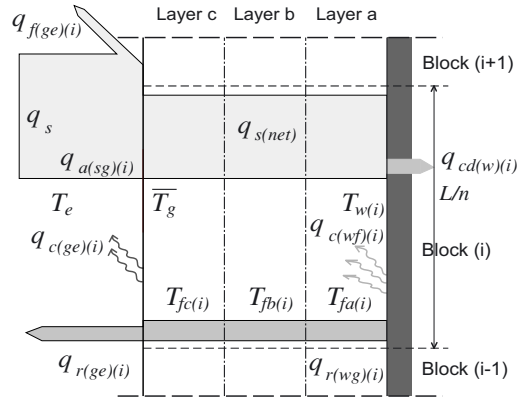

Figure 2. Energy transfers in the block model

Heat balance for a given block of wall:

$$q_{a(sw)(i)} = q_{c(wf)(i)} + q_{r(wg)(i)} + q_{cd(w)(i)} \quad (12)$$

Absorbed solar energy:

$$q_{a(sw)} = q_{s(net)}\alpha_w \quad (13)$$

Convective heat loss to the flowing fluid:

$$q_{c(wf)(i)} = h_{(wf)(i)}\left(T_{w(i)} - T_{f(i)}\right) \quad (14)$$

Conductive heat loss through the backside insulation:

$$q_{cd(w)(i)} = U_b(T_{w(i)} - T_b) \quad (15)$$

Radiation heat loss to the glazing:
$q_{r(wg)(i)}$: same as equation (11).

Ventilation rate equations
When calculating the flow rate of the chimney, ventilation flow rate for each layer is calculated separately and then summarized to get the overall flow rate of the chimney.
Densities in layer (a):
Average: $\overline{\rho_a} = 353.25/\overline{T_{fa}}$
Outlet: $\rho_{fa(n)} = 353.25/T_{fa(n)}$
Flow rate equations for layer (a):
At the outlet:

$$Q_{oa} = C_{do}A_a\sqrt{\frac{2}{\rho_{fa(n)}}\left[\left(\rho_e - \overline{\rho_{fa}}\right)gLsin\varphi + p_m\right]} \qquad (16)$$

At the inlet:

$$Q_{ia} = C_{di}A_a\sqrt{\frac{2}{\rho_r}\left(-p_m\right)} \qquad (17)$$

A simulation program can be constructed using these equations to simulate the heat transfer and the airflow in the chimney.

Experiments
Experimental setup
Experiments were conducted to provide measurement data for the simulation model. A flexible experimental apparatus was constructed so that the most of the variables could be changed during the experiments. The experimental apparatus is a chimney channel with changeable channel thickness and inclination angle. Electrically heated panels below the aluminum wall surface provided the heat flux. The backside was heavily insulated. Length of the channel was 2 m, the width 1 m. Channel thickness was changed between 10, 20 and 30 cm. The inclination of the chimney was 30, 45, 60, 75 and 90 degrees. Heat flux was 100, 300 or 500 W/m². The experimental arrangement can be seen on Figure 3.
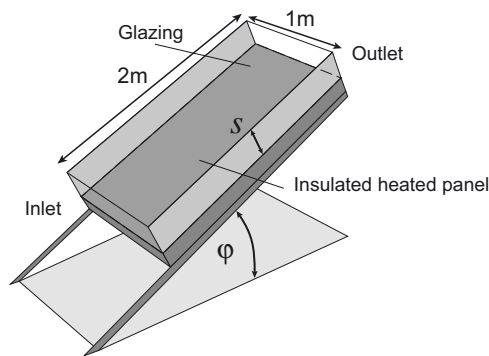

Figure 3. Experimental apparatus

Measurement techniques
The measurements were carried out in a high-ceiling experimental room. Room temperature was maintained between 13 and 16 degrees during the experiments. Measurements were carried out when the apparatus reached thermal stability with the environment.
The backside heat loss, wall temperature and air temperature, as well as room temperature were measured using thermocouples. The outlet velocities were measured with a hot-wire anemometer at the outlet, in matrix arrangement.

Results and discussion
Characteristic variables and conditions
The values of the variables used or measured during the experiments and the input variables of the simulation are corresponding to each other, and their numerical values are shown in Table 1. Conditions of the experiment can be seen on Table 2.

Table 1. Characteristic variables

Variable	Value
Chimney width w [m]	1
Chimney height L [m]	2
Number of blocks n [-]	20
Inlet discharge coefficient C_{di} [-]	0.8
Outlet discharge coefficient* C_{do} [-]	
s=0.1 m	1.5
s=0.2 m	2.1
s=0.3 m	2.7
Ambient temperature T_e [K]	288

*Channel friction resistance is considered

Table 2. Experiment conditions

$q_{s(net)}$ (W/m²)		100	300			500
s (cm)		20	10	20	30	20
φ(°)	30			O		
	45			O		
	60	O	O	O	O	O
	75			O		
	90			O		

Experimental and simulation results
Flow rate versus heat flux
Figure 4 shows the relation between heat flux and mass flow rate. The results show that the flow rate is highly dependent on the heat flux. Even at small heat fluxes sufficient flow rates are produced. At the incident heat flux of 100 W/m² more than the half of the flow rate of 500 W/m² was generated.
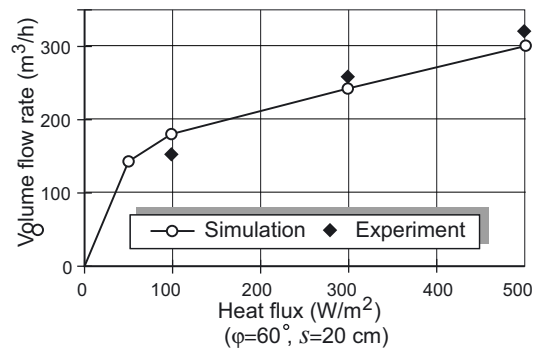

Figure 4. Flow rate and heat flux

Inclination versus flow rate
Figure 5 shows the relation between these variables. Maximum flow rate was observed at 45 degrees. The smaller flow rates at bigger inclination angles occurred because even if the buoyancy effect grew due to the bigger inclination, the thinner boundary layer resulted in smaller flow rate. Simulation data is matching well with the experimental, although at 90 degrees the results are a bit different. Increasing the number of layers could give more accurate results here.
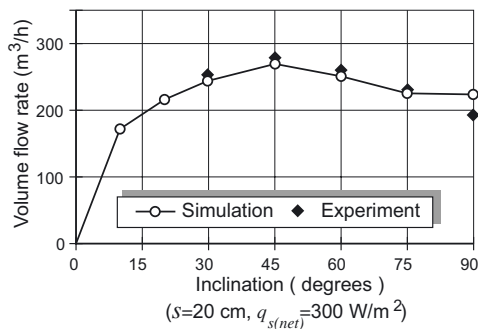

Figure 5. Inclination and flow rate

Channel thickness versus flow rate
Figure 6 shows the relation of these variables. The increment in the channel thickness means a decrease of the resistance for spreading the heat in the channel. As heat spread results thicker boundary layer, this causes the larger flow rates mentioned above.
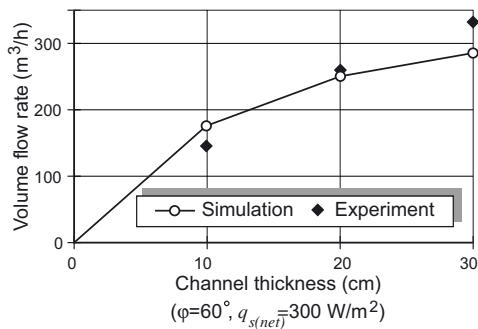

Figure 6. Channel thickness and flow rate

Conclusion
The simulation model is able to predict flow rates for a wide range of variables. There are some differences, which can later be eliminated using more accurate equations to calculate the boundary layer thickness and the local heat transfer coefficients. As usual solar chimneys are vertical or inclined over 45 degrees, the model is very useful to simulate chimney performance.

Nomenclature
Geometrical variables

L	length of the chimney [m]
s	distance between wall and glazing [m]
φ	inclination of the chimney [°]
w	width of the chimney [m]
A	inlet and outlet opening area [m^2]
C_{di}, C_{do}	inlet and outlet discharge coefficient [-]
n	number of blocks [-]

Physical variables

α, ε, τ	absorbtance, emittance, transmittance [-]
F	radiation shape factor [-]
U_b	overall rear conductive heat transfer coefficient at the wall [W/m^2K]
c_p, ν, k	specific heat [J/kgK], dynamic viscosity [m^2/s], and heat conductivity [W/m^2K] of air
β	volume coefficient of expansion [1/K]
T	temperature [K]
h	heat transfer coefficient [W/m^2K]
q	heat flux [W/m^2]
m	mass flow rate [kg/s]
σ	Stefan-Boltzmann constant [W/m^2K^4]
g	acceleration of gravity [m/s^2]

Subscripts

s, r, c, cd, a	solar, radiation, convective, conductive, absorbed energy
(wf), (wg), (ge)	wall to fluid, wall to glazing, glazing to environment
w, g, f, e	wall, glazing, fluid and environment.
a, b, c	layer number
(i)	block number

References
Bansal, N.K.; Mathur, R.; Bhandari, M.S. 1993. Solar chimney for enhanced stack ventilation. Building and Environment, Vol. 28, No. 3, pp 373-377.
Sandberg, M.; Mosfegh, B. 1996. Investigation of fluid flow and heat transfer in a vertical channel heated from one side by PV elements. Proceedings of The Fourth Renewable Energy Congress, Denver, USA, (1996)
Alfonso, C.; Oliveira, A. 2000. Solar chimneys: simulation and experiment. Energy and Buildings, Vol. 32, No. 1, pp71-79.
Katsuto, Y. 1964. Heat transfer (in Japanese). Tokyo: Yokendo
Holman, J.P. 1997. Heat transfer. New York: McGraw-Hill.